Check for updates

Comparing two cortisol aptamers for label-free fluorescent and colorimetric biosensors†

Chenqi Niu,[ab] Yuzhe Ding,[b] Chong Zhang[*a] and Juewen Liu [iD] [*b]

Cortisol is a stress hormone and abnormal secretion of cortisol is related to many chronical diseases and neurological disorders. To detect cortisol, two DNA aptamers have been reported so far: 15-1 and CSS.1. In this work, two truncated aptamers were compared: 40-mer 15-1a and 42-mer CSS.1 using isothermal titration calorimetry, where only CSS.1 showed binding with a K_d of 245 nM. We then explored the label-free fluorescence and colorimetric detection methods of cortisol. Using SYBR Green I to stain the aptamers, CSS.1 showed 53% saturated fluorescence enhancement, and this assay allowed us to conclude that its binding was independent of Na^+ and only weakly dependent on Mg^{2+}. Moreover, two mutants and three truncated aptamers of CSS.1 were evaluated. In addition, cortisol had no effect on the colloidal stability of gold nanoparticles (AuNPs) and did not affect DNA adsorption by AuNPs, allowing a colorimetric assay of cortisol binding. While a cortisol-dependent color change was observed, this assay was interfered by other molecules that can cause aggregation of AuNPs such as dopamine. Since none of these assays showed cortisol binding with the truncated 15-1a aptamer, we concluded that 15-1a cannot bind to cortisol, and a more careful truncation study on the original aptamer is needed.

Introduction

Cortisol is a stress hormone secreted by the adrenal gland during psychological or physical stresses.[1] Cortisol is the end-product of the hypothalamic–pituitary–adrenal (HPA) axis.[2] The accumulation of cortisol increases the concentrations of fat and amino acids, which can lead to many diseases (*e.g.*, Cushing's disease, autoimmune disease, cardiovascular complications, and type 2 diabetes) and neurological disorders (depression and anxiety disorders).[3,4] In contrast, abnormally low cortisol levels can lead to Addison's disease, which results in hypercholesterolemia, weight loss, and chronic fatigue.[4] The serum total cortisol concentrations in COVID-19 patients were higher than those in patients without the infection.[5] Therefore, methods for measuring cortisol levels have been extensively developed over the past decade to quantitatively analyze stress levels.

While immunoassays have been used for the detection of cortisol in serum,[6–8] these assays are in a competitive format and thus are signal-off sensors. In this regard, aptamer-based biosensors have the advantage of producing signal-on sensors.[9,10] In addition, DNA aptamers are more stable, more cost-effective, and more consistent than antibodies.[11–13] So far, two DNA aptamers for cortisol have been reported. In 2014, Martin *et al.* reported a full-length 85-nucleotide (nt) aptamer, and the random region contained 40-nt.[14] Using microscale thermophoresis, its K_d was determined to be 16.1 μM, which was comparable with the 6.9 μM K_d obtained from equilibrium dialysis. Many subsequent biosensor studies used the full-length aptamer,[15–19] while some also used only the 40-nt random region, although rigorous binding assays to confirm binding of the truncated aptamer have yet to be performed.[20–23]

In 2017, the Stojanovic group selected a few high-affinity aptamers for steroids, including cortisol and they bind with K_d's ranging from 30 nM to 140 nM.[24] These aptamers were much less used for biosensors probably because they were reported later.[25] We noticed that both aptamer selection experiments were performed by the immobilization of the DNA libraries,[9,26–30] although the library design was different.

Label-free aptamer biosensors are attractive since they are cost-effective.[31–34] At the same time, they can also offer fundamental insights into aptamer binding reactions. Two types of label-free biosensors are very common. One type uses DNA staining dyes such as SYBR Green I (SGI) and thioflavin

ᵃ MOE Key Laboratory for Industrial Biocatalysis, Institute of Biochemical Engineering, Department of Chemical Engineering, Tsinghua University, Beijing, 100084, China. E-mail: chongzhang@mail.tsinghua.edu.cn
ᵇ Department of Chemistry, Waterloo Institute for Nanotechnology, University of Waterloo, 200 University Avenue West, Waterloo, Ontario N2L 3G1, Canada. E-mail: liujw@uwaterloo.ca

T, resulting in a fluorescence intensity change upon target binding.[34,35] The other type uses gold nanoparticles (AuNPs).[36] For this method to work, it is important to study the interaction between AuNPs and cortisol. If they interact strongly, AuNP-related biosensors (e.g. surface plasmon resonance, surface-enhanced Raman scattering, and even electrochemistry with gold electrodes) need to consider such interactions.[31] While AuNP-based detection has also been used for the cortisol aptamers,[15,20] little was known regarding the interaction between cortisol and AuNPs.

In this work, we aimed to achieve three related goals. First, we compared these two aptamers side-by-side using a range of binding assays. Second, we studied the interaction between cortisol and AuNPs and tested whether the AuNP-based label-free colorimetric assay can be applied for the detection of cortisol or not. Finally, we also studied a fluorescent label-free biosensor and used it to understand the binding properties of the aptamers.

Materials and methods

Chemicals

All of the DNA samples were purchased from Integrated DNA Technologies (IDT, Coralville, IA). The sequences and modifications of the DNAs are listed in Table S1.† Cortisol, deoxycholic acid, 17β-estradiol, thymidine and dopamine were purchased from Sigma-Aldrich. Citrate-capped AuNPs (13 nm) were prepared based on the literature method, and the as-prepared AuNPs were ~10 nM.[37] Milli-Q water was used for preparing buffers and solutions.

Buffers

To study aptamer binding under different conditions, a number of buffers were prepared. Buffer 1 (the buffer used for selecting the CSS.1 aptamer): 20 mM HEPES (pH 7.5), 5 mM KCl, 1 M NaCl and 10 mM MgCl₂. Buffer 1-1: 20 mM HEPES (pH 7.5), 5 mM KCl, 100 mM NaCl and 10 mM MgCl₂. Buffer 1-2: 20 mM HEPES (pH 7.5), 5 mM KCl, 100 mM NaCl and 2 mM MgCl₂. Buffer 1-3: 20 mM HEPES (pH 7.5), 5 mM KCl and 100 mM NaCl. Buffer 2 (the buffer used for selecting the 15-1 aptamer): 50 mM HEPES (pH 7.5), 137 mM NaCl and 5 mM MgCl₂. Buffer 3 (the buffer used for avoiding the adsorption of HEPES on AuNPs): 10 mM phosphate (pH 7.5) and 1 mM MgCl₂. Artificial interstitial fluids (ISF): 2.5 mM CaCl₂, 10 mM HEPES, 3.5 mM KCl, 0.7 mM MgSO₄, 123 mM NaCl, 1.5 mM NaH₂PO₄, 7.4 mM sucrose, pH 7.5.[38]

Isothermal titration calorimetry (ITC) assays

ITC was performed using a VP-ITC microcalorimeter instrument (MicroCal) following previously reported procedures.[30] Prior to each measurement, all of the solutions were degassed for 5 min to remove air bubbles. DNA aptamer (5 μM) in buffer was loaded in the ITC cell (1.45 mL) at 25 °C. Cortisol (100 μM) in the same buffer was titrated (20 μL each time) into the cell through a syringe, except for the first injection (2 μL). The enthalpy (ΔH) and association constant K_a were obtained by fitting the titration curves to a one-site binding model using the Origin software. Buffer 1, 1-1, 1-2, and 1-3 were used for CSS.1-related aptamers. Buffer 2 was used for 15-1-related aptamers.

Label-free fluorescence binding assays

The 500 μL reaction containing 1× buffer, 5 μM aptamer, 0.5× SGI dye and various concentrations of cortisol. Fluorescence spectra with 522 nm excitation were measured using a Varian Eclipse fluorimeter. Buffer 1-1, 1-2, 1-3, and 3 and ISF were used for CSS.1-related aptamers. Buffer 2 was used for 15-1-related aptamers. The K_d values were obtained by fitting the curve using the equation $F = F_{max}X/(K_d + X) + F_0$, where F is the measured fluorescence intensity, F_{max} is the maximum fluorescence intensity, X is the cortisol concentration, and F_0 is the measured background fluorescence without cortisol.

Cortisol adsorption by AuNPs

To evaluate the effect of cortisol on the colloidal stability of AuNPs, 35 μL AuNPs (13 nm, 10 nM) were mixed with 5 μL various concentrations of cortisol, 50 μL 2× buffer 3 (20 mM phosphate, 2 mM MgCl₂, pH 7.5) and 10 μL Milli-Q water. After incubation for 5 min, the UV-vis spectra and photographs were taken. To evaluate the adsorption of cortisol by AuNPs, 35 μL AuNPs were first mixed with 5 μL cortisol of different concentrations in 50 μL 2× buffer 3. After incubation for 5 min, 5 μL FAM-DNA (4 μM) was introduced. After 5 min incubation, 5 μL NaCl (1.3 M) was added followed by 5 min incubation. The resulting mixture was then centrifuged and washed three times to remove the free DNA, and the supernatant was collected and diluted 20 times with buffer 3. The fluorescence intensity with 522 nm excitation was measured (F_1). The precipitation was resuspended with buffer 3 to 99 μL. After being treated with 1 μL KCN (final 1 mM), the solution was diluted 20 times with buffer 3 and its fluorescence intensity was recorded as F_2. The fraction of DNA adsorption by AuNPs was calculated to be $F_2/(F_1 + F_2)$.

AuNP-based label-free colorimetric assays

To evaluate the performance of aptamers with the typical aptamer-based colorimetric detection method, 5 μL aptamer (4 μM) was first mixed with 5 μL cortisol of different concentrations in 50 μL 2× buffer 3. After incubation for 5 min, 35 μL AuNPs were introduced. After incubation for 5 min, 5 μL NaCl (1.3 M) was added. After incubation for 5 min, the UV-vis spectra were acquired and photographs were taken.

Results and discussion

The two cortisol aptamers

Both of the previously reported cortisol aptamers were isolated using the library-immobilization selection method,[14,24] with the random regions containing 40- or 30-nt. A careful comparison of the secondary structures of the libraries revealed a major
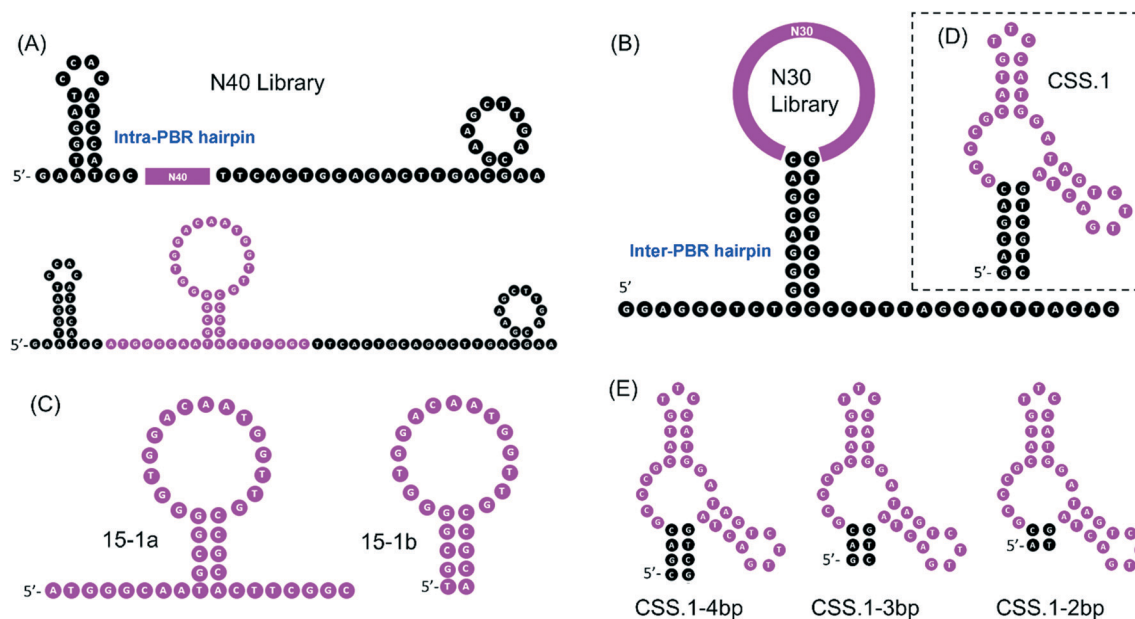
Fig. 1 The library design for the previous aptamer selection experiments with (A) intra- and (B) inter-PBR hairpins. (C) The truncated 40-mer sequence 15-1a and the further truncated 25-mer sequence 15-1b. The secondary structures of (D) CSS.1, and its truncated (E) CSS.1-4bp, CSS.1-3bp and CSS.1-2bp.

difference in the library design in the fixed primer binding regions (PBRs). The library used by Martin *et al.* had an intra-PBR hairpin (Fig. 1A, the hairpin on the 5′ side of the top panel), while Stojanovic's library had an inter-PBR hairpin (Fig. 1B). During aptamer selection, such hairpins were intended to facilitate cortisol binding sequences to dissociate from the immobilization columns upon target binding. Such a difference was also reflected in the predicted secondary structure of the aptamers. The full-length 15-1 aptamer reported by Martin *et al.* retained the hairpin in its predicted secondary structure, and the central random region seems to form its own structure. So far, truncation to 15-1 was made by simply removing the two PBRs.[14,20] After truncation, the 40-mer sequence (named 15-1a) still has overhangs outside the hairpin. Thus, we also further truncated it to obtain a 25-mer sequence named 15-1b (Fig. 1C). In this work, we only tested the truncated sequences, since it's difficult to use the full-length 85-mer for rational biosensor design.

Based on the secondary structure of the CSS.1 aptamer, the truncation is quite straightforward. If eight base pairs are retained in the aptamer, the length is 46-mer. In this study, we keep six base pairs and the aptamer is 42-mer (Fig. 1D). In addition, three further truncated CSS.1 aptamers were tested, where the stem was shortened from 6 to 4, 3 and 2 base pairs (Fig. 1E). To ensure specificity of binding, we also included two mutants for this study by changing a few nucleotides in the random region of CSS.1 (Fig. S1†).

ITC binding assays

Our first goal was to compare these two aptamers for cortisol binding. To directly study the binding reactions, we performed ITC by titrating cortisol into different aptamers,[39] and the rate of heat release was recorded. For CSS.1, the reaction was exothermic as indicated by the downward spikes of the thermograms in Fig. 2A. After subtracting the background heat, the net heat was integrated and fitted to a one-site binding model (Fig. 2A, the lower panel), from which the dissociation constant (K_d) was calculated to be 245 ± 39 nM, indicating the binding of cortisol with CSS.1. This value was comparable with the 100 nM K_d from the fluorescence-based DNA strand displacement assay reported previously.[24] To further confirm the binding, two mutants of CSS.1 were designed (CSS.1-mt1: G7A and A24G double mutant and CSS.1-mt2: G7T, see Fig. S1†), which showed no binding (Fig. 2B and C). Thus, the G7 base in CSS.1 was critical for the binding. We then titrated cortisol into the 15-1a aptamer, but no binding was observed (Fig. 2D). In order for the binding to take effect, we doubled the concentration of the aptamer to 10 μM (Fig. S2†), but still no heat change was observed, indicating no binding between cortisol and 15-1a.

Salt-dependent binding

Salt concentration is essential to the interaction between aptamers and targets, and it is also critical for biosensors. For example, the binding of SGI and DNA is strongly affected by salt,[40] and the colloidal stability of AuNPs is also determined by salt.[41] 1 M NaCl was used in the selection of the CSS.1 aptamer. To test for physiologically relevant conditions, 100 mM NaCl solutions with different concentrations of Mg^{2+} were investigated (Fig. 3). Compared with 1 M NaCl in Fig. 2A, 100 mM NaCl resulted in a slightly higher K_d of 656 ± 19 nM, which indicated that lowering the concentration of Na^+ did not have a
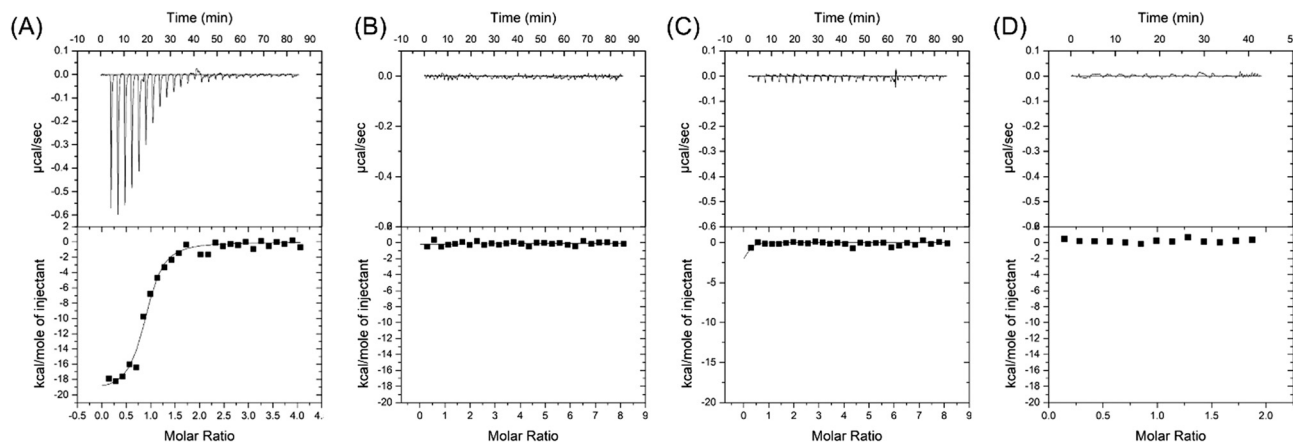
Fig. 2 Comparison of the two aptamers and their mutants using ITC: (A) CSS.1; (B) CSS.1-mt1; (C) CSS.1-mt2; (D) 15-1a. Buffer 1 was used in (A)–(C) and buffer 2 was used in (D). These buffers were used for the selection of these aptamers.

strong effect on the affinity between the aptamer and cortisol (Fig. 3A). By fixing the NaCl concentration at 100 mM, we further dropped the Mg^{2+} concentration. The K_d was 1.9 ± 0.9 μM and 4.9 ± 0.7 μM in the buffer with 2 mM Mg^{2+} and no Mg^{2+}, respectively (Fig. 3B and C). A K_d of 4.9 μM is still quite good for a small molecule. For example, the classic adenosine aptamer has a K_d of around 6 μM in a buffer containing Mg^{2+}.[42] Therefore, Mg^{2+} was not required for the binding, but it was helpful to achieve a higher binding affinity.

Fluorescence label-free detection of cortisol

After confirming the binding of the CSS.1 aptamer, we then used a DNA staining dye to develop a label-free sensor, which allowed us to further evaluate the binding of the aptamers. As shown in Fig. 4A, aptamer binding to cortisol may

promote the formation of the hairpin structure, leading to enhanced SGI fluorescence. In buffer 1-1 containing 100 mM Na^+ and 10 mM Mg^{2+}, the fluorescence intensity indeed increased with the increase of cortisol concentration (Fig. 4B). The same phenomenon was observed in other buffers (Fig. 4C). The K_d increased from 4.7 μM to 15.4 μM with the concentration of Mg^{2+} decreasing from 10 mM to 0. This trend was consistent with that in the ITC assay. However, the K_d values in the SGI assay were higher (by 1.8 to 7.2 times) than those in ITC, which could be due to SGI acting as a competitor for aptamer binding.

Moreover, the two mutated aptamers, CSS.1-mt1 and CSS.1-mt2, were investigated (Fig. 4D). As expected, these mutants did not lead to a fluorescence intensity increase consistent with the ITC results. We further truncated the three truncated CSS.1 aptamers (Fig. 1E), and the aptamers
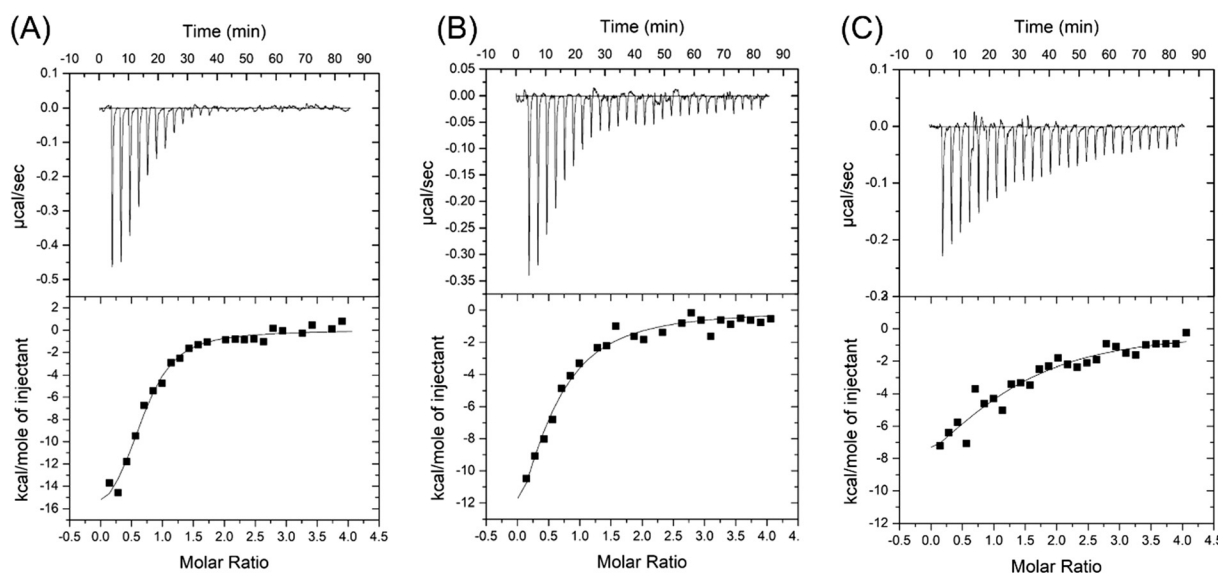

Fig. 3 Effect of the salt concentration on the CSS.1 aptamer. (A) 100 mM NaCl and 10 mM $MgCl_2$. $K_d = 656 \pm 19$ nM. (B) 100 mM NaCl and 2 mM $MgCl_2$. $K_d = 1.9 \pm 0.9$ μM. (C) 100 mM NaCl. $K_d = 4.9 \pm 0.7$ μM. Buffer 1-1, buffer 1-2 and buffer 1-3 were used in (A)–(C), respectively.
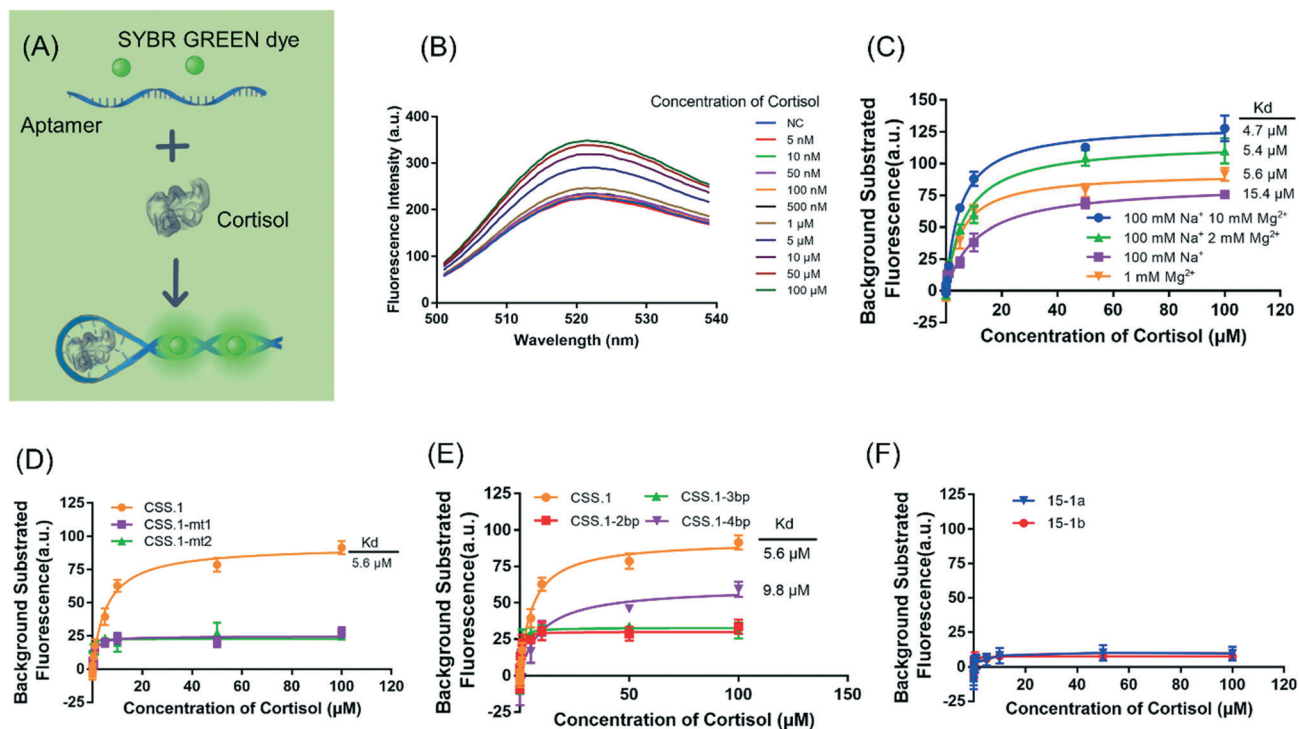
Fig. 4 (A) Schematic of the SGI-based label-free fluorescent assay. (B) Fluorescence spectra of 5 μM CSS.1 mixed with 0.5× SGI in the presence of different concentrations of cortisol. (C) Effect of the salt concentration on the CSS.1 aptamer. (D) Performance of the CSS.1 mutants. (E) Performance of the truncated CSS.1 aptamers. (F) Performance of the 15-1a and 15-1b aptamers. The error bars indicate the standard deviation.

with a shorter stem length had a lower affinity for cortisol (Fig. 4E). The K_d of CSS.1-4bp was 9.8 μM, 1.75-times that of CSS.1, whereas CSS.1-3bp and CSS.1-2bp showed a negligible fluorescence change. Therefore, a minimum of 4bp was required for this label-free sensing method. While 3bp might also bind, such binding could not be probed using SGI. The aptamer binding requires closing of the hairpin and thus if the stem region is too short, the correct binding structure cannot form. Our current CSS.1 aptamer has a 6bp stem, which is sufficiently stable under physiological conditions (*e.g.* 100 mM Na$^+$; 1 mM Mg^{2+}) with an Mfold predicted melting temperature of 59.4 °C. Finally, we tested the 15-1a

and 15-b aptamers using the SGI assay (Fig. 4F), but no cortisol-dependent fluorescence change was observed, indicating a lack of binding with up to 100 μM cortisol.

Detection of cortisol in artificial interstitial fluids

Since the label-free fluorescence method showed a cortisol-dependent signal change, we then evaluated its performance in artificial interstitial fluids (ISF).[38] Quantitative analysis was performed by monitoring the fluorescence intensity after the addition of various concentrations of cortisol. The resulting plot of fluorescence intensity *versus* cortisol
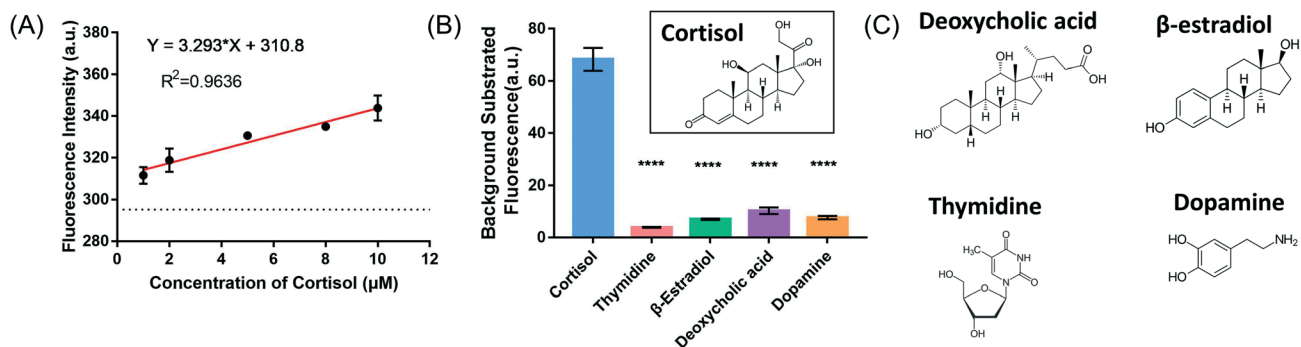

Fig. 5 Detection of cortisol in artificial ISF. (A) The linear range and the regression line. The dashed line indicates the background fluorescence intensity without cortisol. (B) Specificity test with 20 μM cortisol or competing molecules. Inset: The structure of cortisol. The error bars indicate the standard deviation. ****: $P < 0.0001$. (C) The structures of the tested competing molecules.

concentrations was linear over the range of 1 μM to 10 μM (Fig. 5A), and the detection limit was determined to be 742 nM. Moreover, deoxycholic acid, 17β-estradiol, thymidine and dopamine were used to evaluate the specificity of the detection method, and none of them showed significant fluorescence signal changes (Fig. 5B and C), indicating that the fluorescence change was due to specific cortisol binding.

Adsorption of cortisol onto AuNPs

Finally, we explored the possibility of label-free colorimetric detection using citrate-capped AuNPs.[37,43] With salt addition, AuNPs would aggregate and turn from red to blue color.[43] Upon adsorption of DNA oligonucleotides, the colloidal stability of AuNPs increases making them more resistant to
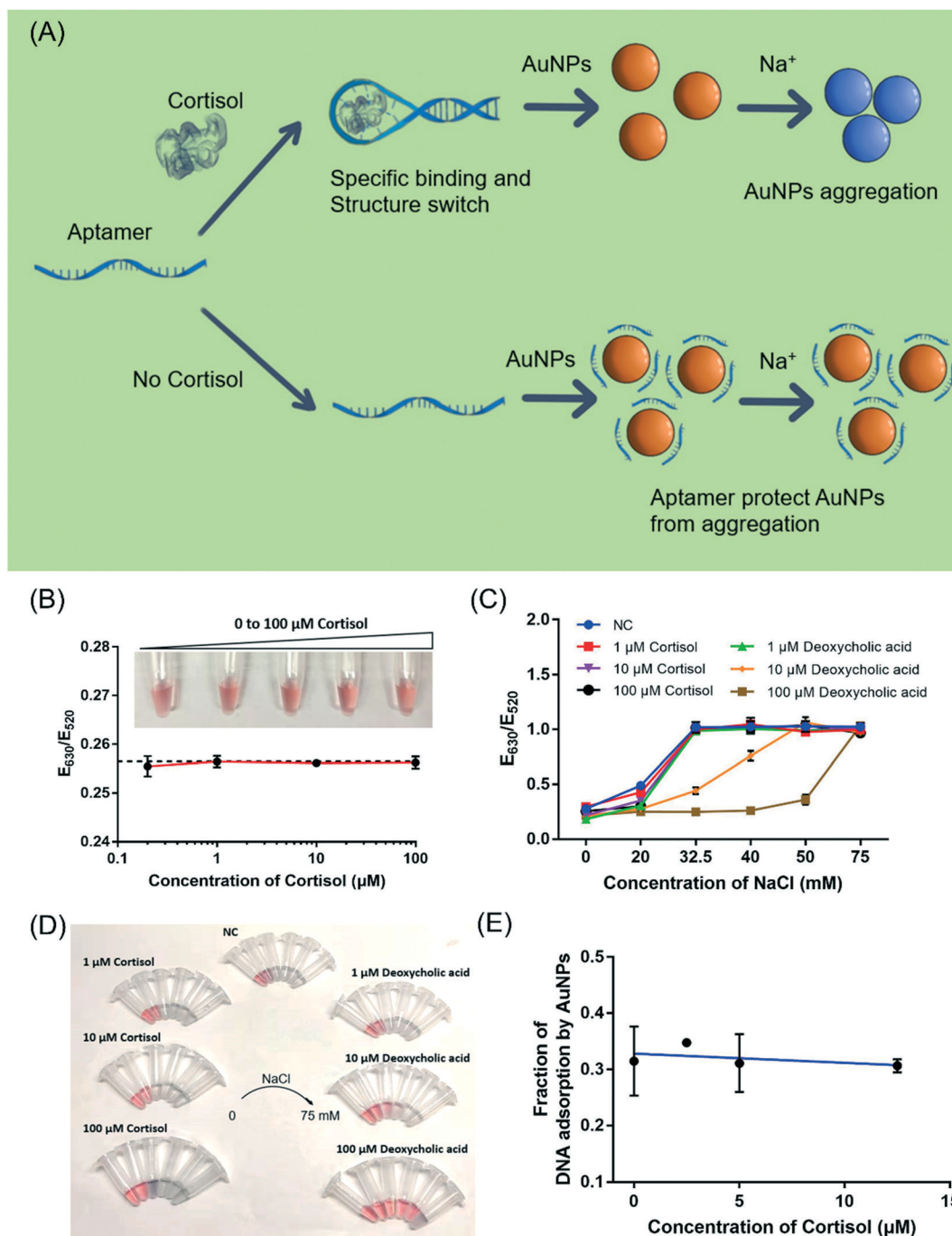

Fig. 6 (A) A scheme showing the aptamer-based colorimetric detection method. (B) Effect of cortisol on the colloidal stability of the AuNPs. The dashed line indicates the E_{630}/E_{520} value without cortisol. Inset: A photograph of the AuNP samples. (C) Effect of cortisol and deoxycholic acid on the salt-resistance of the AuNPs. NC means negative control, where no cortisol or deoxycholic acid was added. (D) Photograph of the data in (C). (E) Effect of cortisol on the adsorption of FAM-labeled DNA. The error bars indicate the standard deviation.

the salt.[36] Most previous work on aptamer-based colorimetric detection assumed a reaction scheme shown in Fig. 6A, where the target molecule induced the folding of the aptamer into a rigid structure and inhibited the adsorption of the aptamer by AuNPs. After adding the salt, the sample turned blue.[31,44,45] In this mechanism, the interaction between the target molecule and AuNPs was not considered. However, as demonstrated for many target analytes, such as adenosine/ ATP,[46] dopamine/melamine,[47] quinine,[48] kanamycin,[49] and Hg^{2+},[50] their adsorption to AuNPs was critical and cannot be ignored.[31]

Therefore, we investigated the interaction between cortisol and the AuNPs. Firstly, the effect of cortisol on the colloidal stability of the AuNPs was studied (Fig. 6B). The 13 nm citrate-capped AuNPs had a strong surface plasmon peak at 520 nm. With the increasing NaCl concentration, the as-prepared citrate-capped AuNPs gradually aggregated and the color turned blue. The onset of the color change was around 32.5 mM NaCl by visual inspection, which was also confirmed by UV-vis measurements (Fig. S3†). With the addition of up to 100 μM cortisol to the AuNPs, the AuNPs remained red, and the E_{630}/E_{520} value indicative of the color of the AuNPs remained constant with cortisol concentrations ranging from 200 nM to 100 μM (Fig. 6B). Thus, either cortisol did not adsorb onto the AuNPs, or the adsorption did not decrease its colloidal stability.

We then investigated the effect of cortisol on the salt-stability of the AuNPs (Fig. 6C and D). The AuNPs aggregated and the color changed to blue by adding 32.5 mM NaCl in the presence of 1 μM, 10 μM and 100 μM cortisol, indicating that the colloidal stability of the AuNPs did not improve. As a control, the effect of deoxycholic acid (a similar structure to cortisol) was also investigated, where the stability of the AuNPs significantly improved. The AuNPs remained red with 32.5 mM NaCl with the protection of 10 μM deoxycholic acid (Fig. 6C, orange trace, orange trace), and they could resist 50 mM NaCl in the presence of 100 μM deoxycholic acid (Fig. 6C, brown trace). Compared to cortisol, deoxycholic acid has a carboxylic acid group, which could be the reason for its adsorption and the stabilization of the AuNPs (a negative

charge). Therefore, deoxycholic acid can improve the stability of the AuNPs by adsorbing on the gold surface, whereas cortisol does not appear to strongly interact with the AuNPs.

Finally, we investigated whether cortisol can affect the adsorption of DNA by AuNPs. Since AuNPs are strong fluorescence quenchers, we used a FAM-labeled DNA (called FAM-DNA) to follow DNA adsorption.[51] Cortisol was first mixed with the AuNPs before adding FAM-DNA. After centrifugation, the adsorbed DNAs were precipitated together with the AuNPs. The fluorescence intensity of the supernatant was compared with the fluorescence intensity from the dissolved pellets (using KCN) to calculate the fraction of DNA adsorption (Fig. 6E). The fraction of the adsorbed DNA did not change with up to 12.5 μM cortisol, indicating that cortisol did not inhibit DNA adsorption by AuNPs. With these experiments, we reason that it might be possible to explore the typical aptamer-based colorimetric detection method presented in Fig. 6A.

Label-free colorimetric detection of cortisol

To test for the label-free colorimetric detection, the NaCl concentration was first optimized to achieve the most sensitive DNA protection (Fig. S4†). Under the optimized conditions, when using the CSS.1 aptamer, the E_{630}/E_{520} value increased modestly with the increasing cortisol concentration from 125 nM to 12.5 μM and the linear range was from 1 μM to 12.5 μM ($R^2 = 0.95$). However, when the nonbinding mutants CSS.1-mt1 and CSS.1-mt2 were used, a E_{630}/E_{520} change was also observed, especially when the cortisol concentration was below 2.5 μM (Fig. 7A). The red-to-blue color change of the two mutant aptamers was also observed (Fig. 7B). Since the color change was quite modest even under the optimized conditions, it was difficult to distinguish specific and nonspecific interactions. Therefore, we cannot conclude that this colorimetric assay can be used for the confirmation of aptamer binding.

Moreover, deoxycholic acid, 17β-estradiol, thymidine and dopamine were used to evaluate the specificity of the AuNP-based assay (Fig. 7C). In the presence of a 100 μM target
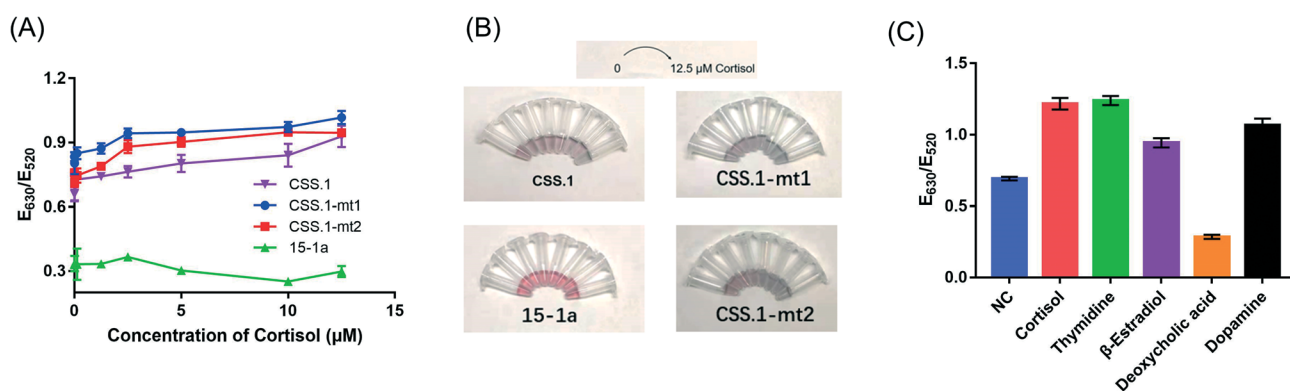

Fig. 7 Evaluation of the AuNP-based label-free biosensor for cortisol. (A) Performance of the different aptamers. (B) Photograph of the data in (A). (C) Specificity test with 100 μM of each molecule. The error bars indicate the standard deviation of the measurements.

molecule, 17β-estradiol, thymidine and dopamine changed the color of the AuNPs from red to blue similar to that with cortisol, while deoxycholic acid retained the red color. These molecules have different interactions with the AuNPs, which in turn affected the colorimetric assay leading to poor specificity. Although a color change was observed with various concentrations of cortisol, we would not call it a sensor for cortisol due to the lack of specificity. Note that the lack of specificity was not due to the aptamer, but due to the interaction between these competing molecules and the AuNPs. This problem might be solved by using organic dyes to produce a color change.[32]

In the presence of various concentrations of cortisol, aptamer 15-1a did not lead to much change in the E_{630}/E_{520} value or AuNP color (Fig. 7A, green trace). So far, we did not find evidence to support the binding of the truncated 40-mer 15-1a aptamer. Thus, the 85-mer full-length aptamer was required for binding (binding was previously confirmed using the microscale thermophoresis (MST),[14] equilibrium dialysis[14] and electrochemical[15] assays). The intra-PBR hairpin in the library also suggested that the PBRs may not be fully removed. Nevertheless, without appropriate truncation and understanding of its minimal secondary structure, it is difficult to use this full-length sequence for rational biosensor design. Given that the CSS.1 aptamer had a much higher affinity than the 15-1 aptamer, researchers are likely to shift their focus on CSS.1 in future research.

Recently, a number of papers have been published to scrutinize the binding of some commonly used aptamers[52] for important analytes such as arsenic,[53] ethanolamine,[54] ampicillin,[55] and some pesticides.[56] None of them showed binding. In this work, another example was discovered. Truncation of aptamers would require a careful test of binding and such binding assays cannot be skipped.

Conclusions

The DNA aptamers for cortisol, 15-1a (a truncated form of 15-1) and CSS.1, were compared side-by-side using ITC, SGI fluorescence spectroscopy and AuNP-based assays. Aptamer 15-1a did not bind to cortisol in any of these assays. Aptamer CSS.1 showed a high binding affinity with a K_d of 245 nM cortisol in its selection buffer. Na$^+$ and Mg^{2+} were not required for CSS.1, but Mg^{2+} was helpful to ensure a high binding affinity. Moreover, two mutant aptamers of CSS.1 were evaluated and the G7 base was essential to ensure aptamer binding. Three truncated aptamers of CSS.1 were also evaluated and the binding affinity decreased with the decreasing stem length of the aptamer. In addition, cortisol had no effect on the colloidal stability of citrate-capped AuNPs and did not affect DNA adsorption. Out of the two label-free assays, the SGI fluorescence assay allowed cortisol detection with a detection limit of 742 nM and showed excellent specificity. However, the AuNP-based colorimetric detection method failed to show a specific color change. Finally, we concluded that the truncated 15-1a aptamer

cannot bind with cortisol, and more systematic and careful truncation work on the original aptamer is needed. Aptamer CSS.1 is an efficient aptamer for cortisol with high tolerance to salt concentration, and it is recommended for future biosensor work.

Conflicts of interest

There are no conflicts to declare.

Acknowledgements

References

1 F. Holsboer and M. Ising, *Annu. Rev. Psychol.*, 2009, **61**, 81–109.

2 A. Levine, O. Zagoory-Sharon, R. Feldman, J. G. Lewis and A. Weller, *Physiol. Behav.*, 2007, **90**, 43–53.

3 D. H. Hellhammer, S. Wüst and B. M. Kudielka, *Psychoneuroendocrinology*, 2009, **34**, 163–171.

4 M. Ku, J. Kim, J.-E. Won, W. Kang, Y.-G. Park, J. Park, J.-H. Lee, J. Cheon, H. Lee Hyun and J.-U. Park, *Sci. Adv.*, 2020, **6**, eabb2891.

5 T. Tan, B. Khoo, E. G. Mills, M. Phylactou, B. Patel, P. C. Eng, L. Thurston, B. Muzi, K. Meeran and A. T. Prevost, *Endocrinology*, 2020, **8**, 659–660.

6 R. Miller, F. Plessow, M. Rauh, M. Gröschl and C. Kirschbaum, *Psychoneuroendocrinology*, 2013, **38**, 50–57.

7 A. Apilux, S. Rengpipat, W. Suwanjang and O. Chailapakul, *J. Pharm. Biomed. Anal.*, 2020, **178**, 112925.

8 J. E. L. Villa, I. Garcia, D. Jimenez de Aberasturi, V. Pavlov, M. D. P. T. Sotomayor and L. M. Liz-Marzán, *Biosens. Bioelectron.*, 2020, **165**, 112418.

9 H. Yu, O. Alkhamis, J. Canoura, Y. Liu and Y. Xiao, *Angew. Chem., Int. Ed.*, 2021, **60**, 16800–16823.

10 A. Ruscito and M. C. DeRosa, *Front. Chem.*, 2016, **4**, 14.

11 L. Wu, Y. Wang, X. Xu, Y. Liu, B. Lin, M. Zhang, J. Zhang, S. Wan, C. Yang and W. Tan, *Chem. Rev.*, 2021, **121**, 12035–12105.

12 Y. Wu, I. Belmonte, K. S. Sykes, Y. Xiao and R. J. White, *Anal. Chem.*, 2019, **91**, 15335–15344.

13 L. He, R. Huang, P. Xiao, Y. Liu, L. Jin, H. Liu, S. Li, Y. Deng, Z. Chen, Z. Li and N. He, *Chin. Chem. Lett.*, 2021, **32**, 1593–1602.

14 J. A. Martin, J. L. Chávez, Y. Chushak, R. R. Chapleau, J. Hagen and N. Kelley-Loughnane, *Anal. Bioanal. Chem.*, 2014, **406**, 4637–4647.

15 B. J. Sanghavi, J. A. Moore, J. L. Chávez, J. A. Hagen, N. Kelley-Loughnane, C.-F. Chou and N. S. Swami, *Biosens. Bioelectron.*, 2016, **78**, 244–252.

16 J. Zhang and S. C. B. Gopinath, *3 Biotech*, 2020, **10**, 35.

17 A. Ganguly, K. C. Lin, S. Muthukumar and S. Prasad, *ACS Sens.*, 2021, **6**, 63–72.

18 R. Zhang and Y. Jia, *ACS Sens.*, 2021, **6**, 3024–3031.

19 M. Pali, B. Jagannath, K.-C. Lin, S. Upasham, D. Sankhalab, S. Upashama, S. Muthukumar and S. Prasad, *Electrochim. Acta*, 2021, **390**, 138834.

20 S. Dalirirad and A. J. Steckl, *Sens. Actuators, B*, 2019, **283**, 79–86.

21 Y. Kim, J. Yang, H. Hur, S. Oh and H. H. Lee, *Biosensors*, 2021, **11**, 163.

22 F. Mortazavi Moghadam, M. Bigdeli, A. Tamayol and S. R. Shin, *Sens. Actuators, B*, 2021, **344**, 130160.

23 Z. Huang, H. Chen, H. Ye, Z. Chen, N. Jaffrezic-Renault and Z. Guo, *Biosens. Bioelectron.*, 2021, **190**, 113451.

24 K.-A. Yang, H. Chun, Y. Zhang, S. Pecic, N. Nakatsuka, A. M. Andrews, T. S. Worgall and M. N. Stojanovic, *ACS Chem. Biol.*, 2017, **12**, 3103–3112.

25 S. Dalirirad, D. Han and A. J. Steckl, *ACS Omega*, 2020, **5**, 32890–32898.

26 R. Nutiu and Y. Li, *Angew. Chem., Int. Ed.*, 2005, **44**, 1061–1065.

27 C. Lyu, I. M. Khan and Z. Wang, *Talanta*, 2021, **229**, 122274.

28 H. Yu, Y. Luo, O. Alkhamis, J. Canoura, B. Yu and Y. Xiao, *Anal. Chem.*, 2021, **93**, 3172–3180.

29 N. Nakatsuka, K.-A. Yang, J. M. Abendroth, K. M. Cheung, X. Xu, H. Yang, C. Zhao, B. Zhu, Y. S. Rim, Y. Yang, P. S. Weiss, M. N. Stojanović and A. M. Andrews, *Science*, 2018, **362**, 319–324.

30 P.-J. J. Huang and J. Liu, *Anal. Chem.*, 2022, 3142–3149, in press.

31 F. Zhang and J. Liu, *Analysis & Sensing*, 2021, **1**, 30–43.

32 O. Alkhamis, J. Canoura, K. V. Bukhryakov, A. Tarifa, A. P. DeCaprio and Y. Xiao, *Angew. Chem.*, 2022, **61**, e202112305.

33 J. Zhang, L.-L. Wang, M.-F. Hou, L.-P. Luo, Y.-J. Liao, Y.-K. Xia, A. Yan, Y.-P. Weng, L.-P. Zeng and J.-H. Chen, *Biosens. Bioelectron.*, 2018, **118**, 1–8.

34 F. Yeasmin Khusbu, X. Zhou, H. Chen, C. Ma and K. Wang, *TrAC, Trends Anal. Chem.*, 2018, **109**, 1–18.

35 L. Kong, J. Xu, Y. Xu, Y. Xiang, R. Yuan and Y. Chai, *Biosens. Bioelectron.*, 2013, **42**, 193–197.

36 H. Li and L. J. Rothberg, *J. Am. Chem. Soc.*, 2004, **126**, 10958–10961.

37 J. Liu and Y. Lu, *Nat. Protoc.*, 2006, **1**, 246–252.

38 P. Bollella, S. Sharma, A. E. G. Cass, F. Tasca and R. Antiochia, *Catalysts*, 2019, 9.

39 S. Slavkovic and P. E. Johnson, *Aptamers*, 2018, **2**, 45–51.

40 H. Zipper, H. Brunner, J. Bernhagen and F. Vitzthum, *Nucleic Acids Res.*, 2004, **32**, e103.

41 B. Liu and J. Liu, *Matter*, 2019, **1**, 825–847.

42 D. E. Huizenga and J. W. Szostak, *Biochemistry*, 1995, **34**, 656–665.

43 J.-W. Park and J. S. Shumaker-Parry, *J. Am. Chem. Soc.*, 2014, **136**, 1907–1921.

44 J. Zhou, Y. Li, W. Wang, Z. Lu, H. Han and J. Liu, *Langmuir*, 2020, **36**, 11490–11498.

45 C. Zong, Z. Zhang, B. Liu and J. Liu, *Langmuir*, 2019, **35**, 7304–7311.

46 F. Zhang, P.-J. J. Huang and J. Liu, *ACS Sens.*, 2020, **5**, 2885–2893.

47 X. Liu, F. He, F. Zhang, Z. Zhang, Z. Huang and J. Liu, *Anal. Chem.*, 2020, **92**, 9370–9378.

48 F. Zhang and J. Liu, *Langmuir*, 2021, **37**, 11939–11947.

49 J. Zhou, Y. Li, W. Wang, Z. Lu, H. Han and J. Liu, *Langmuir*, 2020, **36**, 11490–11498.

50 Y. Hu, Z. Huang, B. Liu and J. Liu, *ACS Appl. Nano Mater.*, 2021, **4**, 1377–1384.

51 X. Zhang, M. R. Servos and J. Liu, *Langmuir*, 2012, **28**, 3896–3902.

52 Y. Zhao, K. Yavari and J. Liu, *TrAC, Trends Anal. Chem.*, 2022, **146**, 116480.

53 C. Zong and J. Liu, *Anal. Chem.*, 2019, **91**, 10887–10893.

54 Y. Ding, X. Liu, P.-J. J. Huang and J. Liu, *Analyst*, 2022, **147**, 1348–1356.

55 F. Bottari, E. Daems, A.-M. de Vries, P. Van Wielendaele, S. Trashin, R. Blust, F. Sobott, A. Madder, J. C. Martins and K. De Wael, *J. Am. Chem. Soc.*, 2020, **142**, 19622–19630.

56 L. Zara, S. Achilli, B. Chovelon, E. Fiore, J.-J. Toulmé, E. Peyrin and C. Ravelet, *Anal. Chim. Acta*, 2021, **1159**, 338382.